Friction Generated Limit Cycles

Ohlsson, Henrik; Åström, Karl Johan

Published in:
IEEE Transactions on Control Systems Technology

DOI:
10.1109/87.930974

2001

Friction Generated Limit Cycles

Henrik Olsson and Karl Johan Åström

***Abstract*—This paper treats limit cycles caused by friction. The goal has been to explain phenomena that have been observed experimentally in mechatronic systems. Experiments have shown that oscillations of qualitatively different types can be obtained simply by changing controller specifications. Stiction is important in some cases but not in others. Necessary conditions for limit cycle are given for the case where stiction is important. Conditions for local stability of the limit cycles are also presented. The results give insight into phenomena observed experimentally.**

***Index Terms*—Friction, limit cycle, relay oscillation, stability.**

I. Introduction

FRICTION is present in all control systems involving mechanical motion and it may cause large steady-state control errors and oscillations. Intuitively oscillations are generated by a combination of friction which counteracts motion and some instability mechanism. In stick-slip motion the mechanism is caused by the desired motion which increases the energy stored in the friction interface. The controller or the process may also be unstable.

This paper was written in order to explain some phenomena that was observed experimentally in [1]. Friction generated limit cycles can be divided into two categories, namely limit cycles with and without sticking. Friction is a very complicated phenomena. Many models of widely different complexity have been developed to describe friction phenomena. A review of a number of models that are appropriate for analysis of control systems are described in [2]. To make the analysis tractable we will consider the situation when there is only one interface where friction occurs. The system can then be described as an interconnection of a linear system and a nonlinear system representing the friction. A particularly simple case is Coulomb friction where the friction model is a static nonlinearity of relay type. This can well describe limit cycles without sticking where the velocity is zero only at isolated time instants. In this case limit cycles can be explained with the theory of relay oscillations [3]–[5]. For oscillations where sticking is important it is necessary to generalize this analysis. This paper is organized as follows. Friction generated limit cycles are discussed and illustrated by an example in Section II. Theory to compute and analyze them are given in Section III. The theory is applied to the example in Section IV. Finally, conclusions are given in Section V.

Manuscript received March 6, 1998; revised January 14, 2000. Manuscript received in final form February 5, 2001. Recommended by Associate Editor K. Kozlowski. This work was supported in part by the Swedish Research Council for Engineering Sciences (TFR) Contract 95–759.

H. Olsson is with the TAC AB, Malmö, Sweden.

K. J. Åström is with the Department of Automatic Control, Lund Institute of Technology, Lund, Sweden (e-mail: kja@control.lth.se).

Publisher Item Identifier S 1063-6536(01)04929-6.

II. Friction Generated Oscillations

In this section we will give some examples of oscillations that are generated by friction. Stick-slip motion is a common phenomena that occurs in slow motion. It can easily be generated in the laboratory by connecting a mass to a spring which is pulled with constant velocity. Stick slip is a jerky motion composed of periods where the surfaces stick and slide. A similar phenomenon can be observed when controlling the position of a sliding mass with a PI controller.

To get some insight into how oscillations are generated we will consider the case when there is only one interface where there is friction. Such a system can be modeled as an interconnection of a linear system and a nonlinear system describing friction. The linear system has the friction force as the input and velocity and possibly the external force as outputs and the friction model has the velocity and possibly the external force as inputs and the friction force as the output. See Fig. 1. The friction interface has an associated relative velocity v, relative position x, friction force F, and external force u. The equation of motion is given by

$$m\frac{d^2x}{dt^2} = m\frac{dv}{dt} = u - F. \tag{1}$$

The motion at the friction interface has thus only one degree of freedom. The friction model we use is

$$F = \begin{cases} F_C \operatorname{sgn}(v) & \text{if } v \neq 0 \\ u & \text{if } v = 0 \text{ and } |u| < F_S \\ F_S \operatorname{sgn}(u) & \text{otherwise.} \end{cases} \tag{2}$$

Viscous friction can be included in the process model and is therefore omitted. The model suffices to analyze most limit cycles qualitatively. In the case of Coulomb friction the friction force is a function only of the velocity as is indicated in Fig. 1(a). In a system with stiction the friction force also depends on the external force, u as shown in Fig. 1(b).

Describing function analysis [6] is a simple approximate method that can be applied to systems of the type shown in Fig. 1(a). [3] has made an exact analysis which is a natural extension of describing function analysis. The only difference is that the describing function is replaced by another curve called the Tsypkin locus. In this way it is possible to obtain necessary conditions for a limit cycle for the case when friction only depends on velocity.

Neither describing functions analysis nor Tsypkin's extension is appropriate when there is sticking because the velocity is zero for intervals of finite lengths. In this case there may be limit cycles of a different nature. Two simple cases are illustrated in Fig. 2. The upper curve represents an oscillation around a desired equilibrium and the velocity changes sign. This type of limit cycle which typically occurs in position control with integral action is called an odd oscillation. The lower curve rep-

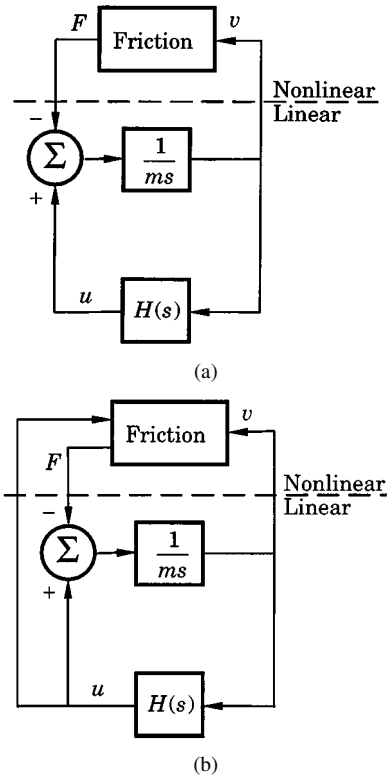

Fig. 1. Describing function analysis where only friction is considered in the nonlinear block.

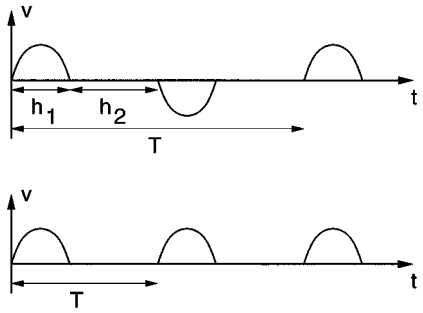

Fig. 2. The characteristics of the velocity for friction limit cycles with sticking. The upper curve shows an odd (bidirectional) limit cycle and the lower curve an even (unidirectional) limit cycle.

resents another type of oscillation where the motion is unidirectional. This type of limit cycle is called an even oscillation. Stick-slip motion is a typical example.

More complicated oscillations where there are several periods of sticking and slipping with different durations have also been observed, see [7]. The analysis in this paper is limited to the types shown in Fig. 2.

There is also a possibility to distinguish between limit cycles that require $F_S > F_C$ and those that exist also for $F_S = F_C$. Stick-slip motion requires that $F_S > F_C$ while the limit cycle in the example below exists also when $F_S = F_C$.

There are dynamic friction models that are more complicated than the simple models with Coulomb friction and stiction, see, e.g., [2]. The simple friction model can, however, explain the limit cycles observed experimentally as discussed in [1] and [8]–[11].

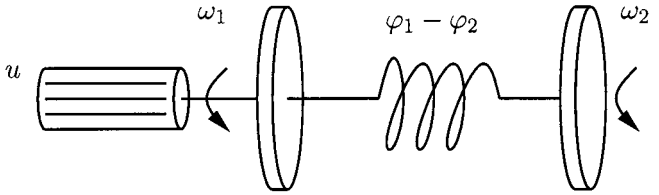

Fig. 3. A schematic picture of the flexible servo.

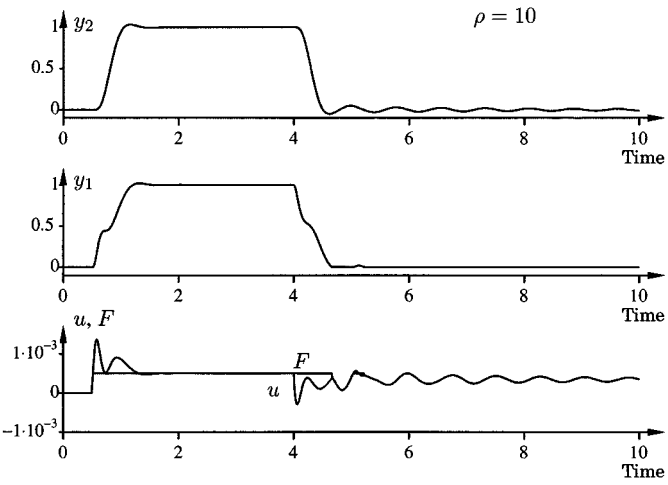

Fig. 4. Simulation of the flexible servo for $\rho = 10$. No limit cycle occurs for this design.

A. An Example

Before proceeding with the analysis we will consider a particular example in more detail. This example is a simulated model which was developed in order to reproduce experiments in [1]. The simulation model described faithfully reproduces the experimental findings. A servo consisting of a motor, a flexible shaft and a load is shown in Fig. 3. The angular velocity of the motor is denoted ω_1 and the velocity of the load ω_2.

We will use numerical values for a system used in the control laboratory, see [12]. The moments of inertia are $J_1 = 2.2 \cdot 10^{-5}$ and $J_2 = 6.0 \cdot 10^{-5}$, the viscous damping coefficients are $d_1 = 3 \cdot 10^{-5}$ and $d_2 = 3 \cdot 10^{-5}$, and $k = 4 \cdot 10^{-4}$ is the stiffness of the shaft. The friction is given by (2) with $F_S = F_C = 5 \cdot 10^{-4}$ and where v corresponds to ω_1, x to φ_1 and m to J_1. We assume that there is friction only on the motor side. The objective is to control the velocity on the load side, i.e., ω_2. The only available measurement is the velocity of the motor $y_1 = k_\omega \omega_1$. The system can be controlled with state feedback and integral action using an observer. The controller gains are chosen to get the desired closed-loop poles which are placed in a Butterworth patterns. The design is specified by the variable ρ, which determines the radius of the Butterworth patterns. The characteristic polynomial is given by $(s^2 + \rho s + \rho^2) \cdot (s^2 + 2\rho \cos(\pi/9)s + \rho^2)(s^3 + 2(2\rho)s^2 + 2(2\rho)^2 s + (2\rho)^3)$.

The behavior of the system changes drastically with the design parameter ρ. Simulations of the responses of the system for $\rho = 10, 11, 12$, and 15 are shown in Figs. 4–7. The diagrams show $y_2 = k_\omega \omega_2$, $y_1 = k_\omega \omega_1$, F and the signal u which is defined by $u = -k(\varphi_1 - \varphi_2) - d_1 \omega_1 + u_c$, where u_c is the torque generated by the controller. The reference velocity is $y_r = 1$

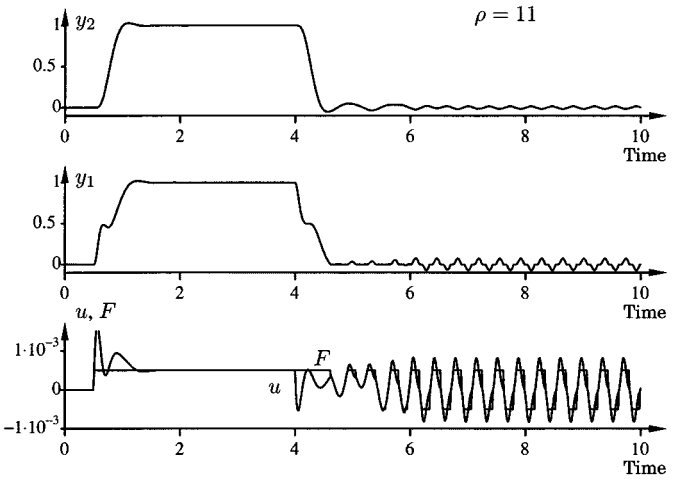

Fig. 5. Simulation of the flexible servo for $\rho = 11$. A limit cycle with periods of sticking occurs.

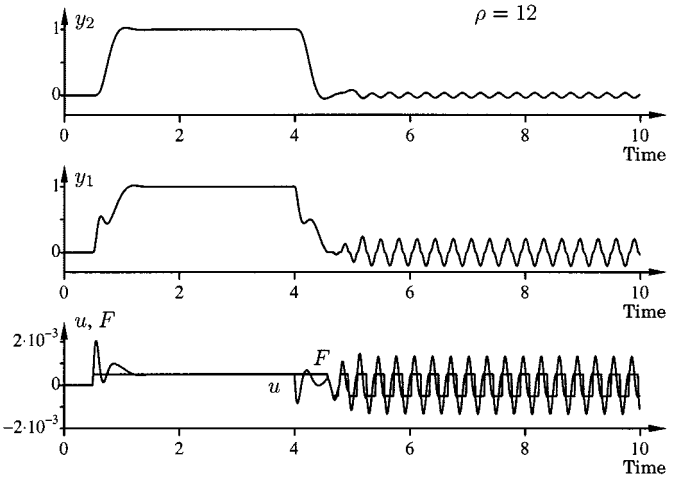

Fig. 6. Simulation of the flexible servo for $\rho = 12$. The limit cycle is a pure relay oscillation with no sticking, i.e., the friction force switches instantly between the levels $\pm F_C$.

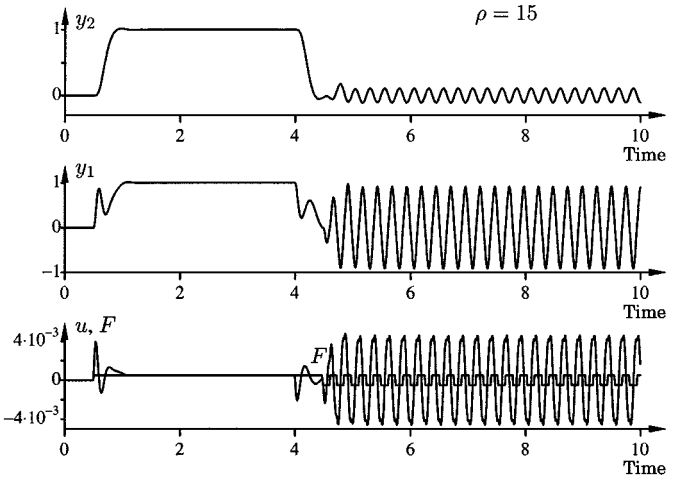

Fig. 7. Simulation of the flexible servo for $\rho = 15$. The limit cycle is a pure relay oscillation, i.e., the friction force switches instantly between the levels $\pm F_C$. The velocity $y_1 = k_\omega \omega_1$ is almost sinusoidal.

between $t = 0.5$ and $t = 4$ and zero otherwise. The controller works properly in all cases until the reference is brought back to zero at $t = 4$. Various limit cycles are then initiated. The measurement y_1 of the velocity for $9 \leq t \leq 10$ are shown in Fig. 8. The behavior obtained in the different cases can be summarized as follows:

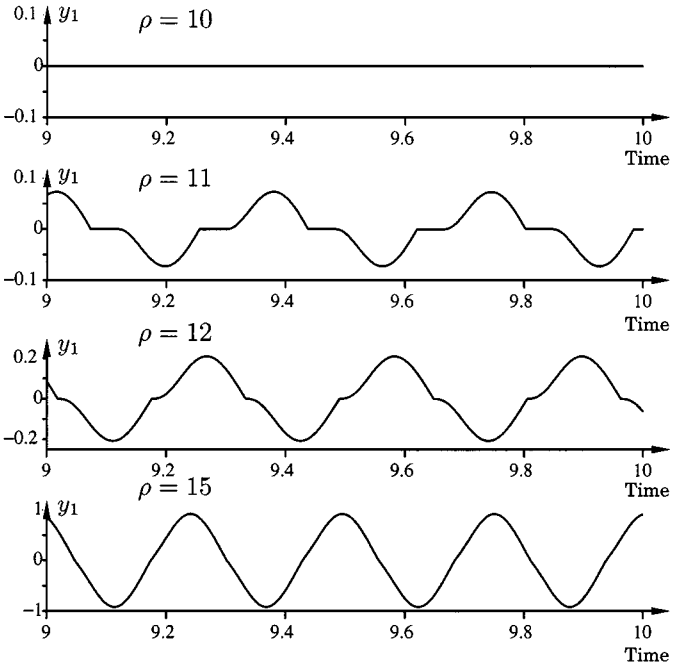

Fig. 8. Close-ups of the oscillatory behavior of the flexible servo for different values of the design parameter ρ. For $\rho = 10$ there is no limit cycle. If $\rho = 11$ we get a limit cycle that includes periods of sticking. For $\rho = 12$ and 5 the velocity is zero only for single time instants.

For $\rho = 10$, the motion of the motor stops soon after $t = 4$. The velocity of the load is then a decaying oscillation. There are no limit cycles.

With $\rho = 11$, a limit cycle with small amplitude is slowly built up after $t = 4$. Fig. 8 reveals that motion stops completely during parts of the limit cycle period.

If $\rho = 12$, the limit cycle becomes an oscillation where the friction force switches instantly between the levels $\pm F_C$. The external force at the times when the velocity becomes zero is sufficiently large to overcome the stiction. The acceleration is, however, quite small immediately after the zero crossings.

When $\rho = 15$, the shape of the velocity $y_1 = k_\omega \omega_1$ is almost sinusoidal. In this case, the external force is much larger than the friction at the times when the velocity is zero.

The behavior of the flexible servo is thus very different for the different values of the design parameter ρ. The mechanism which sustains the oscillation is the controller which is unstable for $\rho = 11, 2$, and 5 but not for $\rho = 10$, in which case no limit cycle was observed.

III. Analysis

In this section we develop an analysis method that permits exact calculation of the shape and the stability of limit cycles with sticking as described in the previous sections. The problem is similar to analysis of limit cycles in systems with relay feedback. The tools developed for that problem in [5] are now generalized to give necessary conditions for oscillations with sticking. The conditions will then be applied to the example. The idea is

to assume that there is an oscillation and investigate the conditions that must hold for limit cycles with sticking.

The technique applies to general linear systems where friction occurs at a single interface where the motion at the friction interface is given by (1) The complete system can be written in the following form:

$$\begin{aligned}\frac{d\xi}{dt} &= A\xi + B(u-F) + B_r y_r \\ v &= C_v\xi \\ u &= -L_u\xi \end{aligned} \tag{3}$$

where L_u is the feedback from measured and estimated states and the state vector partitioned as

$$\xi = \begin{bmatrix} v \\ x \\ \eta \end{bmatrix} \tag{4}$$

where

- x position;
- v velocity at the friction interface;
- η includes all other states of the system, i.e., both controller and process states.

The corresponding partitions of the system matrices are

$$A = \begin{bmatrix} 0 & 0 & 0 \\ 1 & 0 & 0 \\ A_{\eta v} & A_{\eta x} & A_{\eta\eta} \end{bmatrix} \quad B = \begin{bmatrix} \frac{1}{m} \\ 0 \\ B_\eta \end{bmatrix}$$
$$B_r = \begin{bmatrix} 0 \\ 0 \\ B_{r_\eta} \end{bmatrix} \quad C_v = \begin{bmatrix} 1 & 0 & 0 \cdots 0 \end{bmatrix}. \tag{5}$$

Since the complete state vector ξ includes both process and controller states, the signal u contains both control (or actuator) forces and forces from the process itself. The reference y_r is assumed to be constant and the friction model is given by (2).

A. Odd Limit Cycles

We start by investigating odd limit cycles. Fig. 9 shows the principal behavior of the velocity and the external force u for an odd limit cycle. The velocity is zero at the beginning of the periodic solution. The signal u temporarily overcomes the friction force at $t = 0$ and motion begins. It continues until time $t = h_1$ when the velocity becomes zero. At this point motion stops and the velocity then remains zero until the signal u exceeds the static friction force again. This time motion starts in the opposite direction. A complete period consists of four phases, two periods of sliding and two of sticking. By symmetry it is sufficient to study half a period. Between $t = 0$ and $t = h_1$ the velocity is positive and the motion is given by

$$\begin{aligned}\frac{d\xi}{dt} &= (A - BL_u)\xi - BF_C + B_r y_r \\ v &= C_v\xi. \end{aligned} \tag{6}$$

The following boundary conditions hold:

$$C_v\xi(0) = C_v\xi(h_1) = 0.$$

Furthermore it must be required that $C_v\xi(t) > 0$ for $0 < t < h_1$. If this condition is not fulfilled, the velocity becomes zero before $t = h_1$.

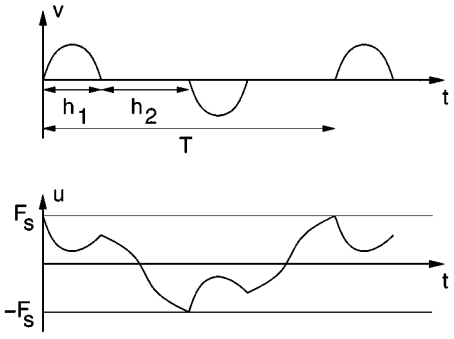

Fig. 9. Velocity and control signal for an odd limit cycle.

In the time interval $h_1 \le t \le h_1 + h_2$ the motion is constrained by the static friction force, which cancels the signal u, see (2), such that the velocity is retained at zero and the position at some constant value. The equation governing this motion is hence

$$\frac{d\xi}{dt} = A\xi + B_r y_r \tag{7}$$

with the boundary condition

$$-L_u\xi(h_1 + h_2) = -F_S.$$

The condition $|L_u\xi(t)| < F_S$ must also hold for $h_1 \le t < h_1+h_2$; otherwise motion would be initiated before $t = h_1+h_2$. For an odd limit cycle we also require that $\xi(h_1+h_2) = -\xi(0)$ because of the symmetry. Necessary conditions for a limit cycle can now be given. The next theorem states conditions in terms of h_1 and h_2 that are necessary for the existence of limit cycles of the type shown in the upper curve of Fig. 2. Candidate values of h_1 and h_2 can be found by solving a nonlinear equation system. Two further constraints on the system solution $\xi(t)$ must also hold. A procedure for applying the theory is given later. We first, however, need to define the following variables:

$$\begin{aligned} A_c &= A - BL_u \quad \Phi_c = e^{A_c h_1} \quad \Phi = e^{Ah_2} \\ \Gamma_c &= \int_0^{h_1} e^{A_c s} ds B \quad \Gamma_{cr} = \int_0^{h_1} e^{A_c s} ds B_r \\ \Gamma_r &= \int_0^{h_2} e^{As} ds B_r. \end{aligned}$$

Note that $\Phi_c, \Gamma_c, \Gamma_{cr}$ are functions of h_1 and that Φ and Γ_r are functions of h_2.

Theorem 1: Consider the system (3) and friction force (2). Assume that there exists an odd periodic solution with period $T = 2(h_1 + h_2)$ and that the matrix $I + \Phi\Phi_c$ is nonsingular. Assume further that the motion is unconstrained in the interval $0 < t < h_1$, but that the friction force keeps the velocity at zero in the interval $h_1 \le t \le h_1 + h_2$ as in Fig. 9. The following nonlinear equations then hold:

$$\begin{aligned} f_1(h_1, h_2) &= C_v(I + \Phi_c\Phi)^{-1} \\ &\quad \cdot (-\Phi_c\Gamma_r y_r - \Gamma_c F_C + \Gamma_{cr} y_r) = 0 \end{aligned} \tag{8}$$

$$\begin{aligned} f_2(h_1, h_2) &= -L_u(I + \Phi\Phi_c)^{-1} \\ &\quad \cdot (-\Phi\Gamma_c F_C + \Phi\Gamma_{cr} y_r + \Gamma_r y_r) = -F_S. \end{aligned} \tag{9}$$

The solution $\xi(t)$ must satisfy

$$v(t) = C_v\xi(t) > 0 \quad \text{for } 0 < t < h_1 \tag{10}$$
$$|u(t)| = |L_u\xi(t)| < F_S \quad \text{for } h_1 \le t < h_1 + h_2. \tag{11}$$

The state vector $\xi(t)$ is for $0 \le t \le h_1$ given by

$$\xi(t) = e^{A_c t}a - \int_0^t e^{A_c(t-s)}dsBF_C + \int_0^t e^{A_c(t-s)}dsB_r y_r$$

and for $h_1 \le t \le h_1 + h_2$ by

$$\xi(t) = e^{A_c(t-h_1)}b + \int_{h_1}^{t-h_1} e^{A(t-s)}dsB_r y_r$$

where

$$a = -(I + \Phi\Phi_c)^{-1}(-\Phi\Gamma_c F_C + \Phi\Gamma_{cr}y_r + \Gamma_r y_r)$$
$$b = (I + \Phi_c\Phi)^{-1}(-\Phi_c\Gamma_r y_r - \Gamma_c F_C + \Gamma_{cr}y_r).$$

The periodic solution is obtained with the initial condition

$$\xi(0) = a = -(I+\Phi\Phi_c)^{-1}(-\Phi\Gamma_c F_C + \Phi\Gamma_{cr}y_r + \Gamma_r y_r) \tag{12}$$

and further the state at time h_1 is given by

$$\xi(h_1) = b = (I + \Phi_c\Phi)^{-1}(-\Phi_c\Gamma_r y_r - \Gamma_c F_C + \Gamma_{cr}y_r). \tag{13}$$

Proof: Integrating the system (6) during the slipping phase with the initial condition $\xi(0) = a$ gives

$$\xi(h_1) = \Phi_c a - \Gamma_c F_C + \Gamma_{cr}y_r. \tag{14}$$

At time h_1 the velocity should be zero, i.e., $v(h_1) = C_v\xi(h_1) = 0$. The constrained motion with zero velocity then continues until time $t = h_1 + h_2$ when the external force overcomes the friction force. Integrating (7) we get

$$\xi(h_1 + h_2) = \Phi\xi(h_1) + \Gamma_r y_r = -\xi(0) = -a \tag{15}$$

since the periodic solution is odd. Solving the equations yields the initial condition (12). The conditions $v(h_1) = 0$ and $u(h_1 + h_2) = -F_S$ are equivalent to (8) and (9). It is further required that $v(t) > 0$ for $0 < t < h_1$, and $|u(t)| < F_S$ for $h_1 \le t < h_1 + h_2$, which gives (10) and (11). ■

Remark 1: Conditions (8) and (10) imply that the derivative of the velocity at $t = h_1^-$ is negative, i.e,

$$\frac{dv}{dt}(h_1^-) = C_v(A_c b - BF_C + B_r y_r) = C_v z < 0$$

and conditions (9) and (11) imply that the derivative of the control signal at $t = h_1 + h_2^-$ is negative, i.e,

$$\frac{du}{dt}(h_1 + h_2^-) = -L_u(-Aa + B_r y_r) = -L_u w < 0.$$

This is also clear from Fig. 9. If these conditions are not satisfied, then (10) and (11) cannot be fulfilled.

Remark 2: The analysis has to be modified slightly to deal with even periodic solutions, see Fig. 2. For this case we have

$$\xi(h_1 + h_2) = \xi(0) \text{ and } u(h_1 + h_2) = -L_u\xi(h_1 + h_2) = F_S$$

which causes some sign changes in the conditions for a periodic solution in Theorem 1. This case is discussed in detail in [8].

Remark 3: Note that if $I + \Phi\Phi_c$ is nonsingular then $I + \Phi_c\Phi$ is also nonsingular. The assumption on regularity is necessary when solving (14) and (15). The condition is trivially fulfilled if both A and A_c are stable matrices as in [13]. However, when, as in our example, integrators are involved, there may be more than one solution if the condition is not satisfied. For the desired solution, the velocity v is zero at both $t = h_1$ and $t = h_1 + h_2$, and the position x at $t = h_1 + h_2$ equals that at $t = h_1$.

B. Reduction of Velocity and Position Equations

In order to overcome the problem indicated in Remark 3 of Theorem 1, it is necessary to include the constraint $v(0) = v(h_1) = 0$ in the solution procedure. For problems where also the position is part of the state we must in the same manner include $x(h_1) = -x(0)$. Inserting $v(0) = v(h_1) = 0$ and $x(h_1) = -x(0)$ in the (14) and (15) and using the knowledge of the structure of A, B, and B_r, as seen in (5), we get

$$\begin{bmatrix} 0 \\ -x(0) \\ \eta(h_1) \end{bmatrix} = \begin{bmatrix} \Phi_{cvv} & \Phi_{cvx} & \Phi_{cv\eta} \\ \Phi_{cxv} & \Phi_{cxx} & \Phi_{cx\eta} \\ \Phi_{c\eta v} & \Phi_{c\eta x} & \Phi_{c\eta\eta} \end{bmatrix} \begin{bmatrix} 0 \\ x(0) \\ \eta(0) \end{bmatrix} - \begin{bmatrix} \Gamma_{cv} \\ \Gamma_{cx} \\ \Gamma_{c\eta} \end{bmatrix} \begin{bmatrix} F_C + \Gamma_{crv} \\ \Gamma_{crx} \\ \Gamma_{cr\eta} \end{bmatrix} y_r \tag{16}$$

$$\begin{bmatrix} 0 \\ -x(0) \\ -\eta(0) \end{bmatrix} = \begin{bmatrix} 1 & 0 & 0 \\ h_2 & 10 & \\ \Phi_{\eta v} & \Phi_{\eta x} & \Phi_{\eta\eta} \end{bmatrix} \begin{bmatrix} 0 \\ -x(0) \\ \eta(h_1) \end{bmatrix} + \begin{bmatrix} 0 \\ 0 \\ \Gamma_{r\eta} \end{bmatrix} y_r. \tag{17}$$

The matrices have been partitioned according to the system structure. There are thus two sets of equations with the single constraint

$$-L_u \begin{bmatrix} 0 \\ -x(0) \\ -\eta(0) \end{bmatrix} = -F_S$$

which corresponds to (9) in Theorem 1. The velocity constraint $v(h_1) = C_v\xi(h_1) = 0$, i.e., (8), has been included in the equations. The first two equations of (17) are trivially fulfilled and the first two equations of (16) can be seen as new constraints on the velocity and the position. We thus obtain two matrix equations for $\eta(0)$ and $\eta(h_1)$, namely the last equation of both (16) and (17). Notice that if $\xi \in R^n$ then $\eta \in R^{n-2}$. The unknowns, $\eta(0)$ and $\eta(h_1)$ are functions of the three variables h_1, h_2, and $x(0)$, i.e.,

$$\eta(h_1) = \Phi_{c\eta x}x(0) + \Phi_{c\eta\eta}\eta(0) - \Gamma_{c\eta}F_C + \Gamma_{cr\eta}y_r$$
$$-\eta(0) = -\Phi_{\eta x}x(0) + \Phi_{\eta\eta}\eta(h_1) + \Gamma_{r\eta}y_r. \tag{18}$$

The new constraints on velocity, position, and control signal are given by

$$\Phi_{cvx}x(0) + \Phi_{cv\eta}\eta(0) - \Gamma_{cv}F_C + \Gamma_{crv}y_r = 0$$
$$\Phi_{cxx}x(0) + \Phi_{cx\eta}\eta(0) - \Gamma_{cx}F_C + \Gamma_{crx}y_r = -x(0)$$
$$-L_u \begin{bmatrix} 0 \\ -x(0) \\ -\eta(0) \end{bmatrix} = -F_S. \tag{19}$$

For the reduced problem we have the following result, where e is used to denote $-x(0)$.

Theorem 2: Assume an odd periodic solution exists with period $T = 2(h_1 + h_2)$ and that $I + \Phi_{\eta\eta}\Phi_{c\eta\eta}$ is nonsingular. The following equations then hold:

$$\begin{aligned} f_1(h_1, h_2, e) =& \Phi_{cvx}e + \Phi_{cv\eta}\alpha\Gamma_{cv}F_C + \Gamma_{crv}y_r = 0 \\ f_2(h_1, h_2, e) =& \Phi_{cxx}e + \Phi_{cx\eta}\alpha\Gamma_{cx}F_C + \Gamma_{crx}y_r + e = 0 \\ f_3(h_1, h_2, e) =& L_u \begin{bmatrix} 0 \\ e \\ \alpha \end{bmatrix} = -F_S \end{aligned} \tag{20}$$

where

$$\begin{aligned} \alpha =& (I + \Phi_{\eta\eta}\Phi_{c\eta\eta})^{-1} \\ & \times \big((\Phi_{\eta x} - \Phi_{\eta\eta}\Phi_{c\eta x})e \\ & + \Phi_{\eta\eta}\Gamma_{c\eta}F_C - \Phi_{\eta\eta}\Gamma_{cr\eta}y_r - \Gamma_{r\eta}y_r\big). \end{aligned} \tag{21}$$

The initial condition is given by

$$\xi(0) = a = \begin{bmatrix} 0 \\ x(0) \\ \eta(0) \end{bmatrix} = \begin{bmatrix} 0 \\ e \\ \alpha \end{bmatrix} \tag{22}$$

and the state at $t = h_1$ by

$$\xi(h_1) = b = \begin{bmatrix} 0 \\ -x(0) \\ \eta(h_1) \end{bmatrix} = \begin{bmatrix} 0 \\ -e \\ \beta \end{bmatrix} \tag{23}$$

where

$$\begin{aligned} \beta =& (I + \Phi_{c\eta\eta}\Phi_{\eta\eta})^{-1} \\ & \times \big(-(\Phi_{c\eta x} - \Phi_{c\eta\eta}\Phi_{\eta x})e \\ & - \Gamma_{c\eta}F_C - \Phi_{c\eta\eta}\Gamma_{r\eta}y_r + \Gamma_{cr\eta}y_r\big). \end{aligned} \tag{24}$$

Furthermore, it is necessary that

$$v(t) = C_v\xi(t) > 0 \quad \text{for } 0 < t < h_1$$

and

$$|u(t)| = |L_u\xi(t)| \le F_S \quad \text{for } h_1 \le t < h_1 + h_2$$

where $\xi(t)$ is given in Theorem 1.

Proof: Equation (20) follows directly from (19). Equation (21) and (24) can be obtained by solving (18). ■

Remark 1: It is necessary to have numerical procedures to find the values of h_1, h_2 and e that satisfy (20). The partial derivatives of these functions with respect to the three variables are useful in this respect. These are given in [8].

Remark 2: If the position x is not part of the state vector then the following two conditions suffice:

$$\begin{aligned} f_1(h_1, h_2) =& \Phi_{cv\eta}\alpha - \Gamma_{cv}F_C + \Gamma_{crv}y_r = 0 \\ f_2(h_1, h_2) =& L_u \begin{bmatrix} 0 \\ \alpha \end{bmatrix} = -F_S \end{aligned}$$

with α given by (21) with $e = 0$.

C. Stability of the Limit Cycle

Local stability of the limit cycle can be determined by calculating the Jacobian of a Poincaré map [14]. This map describes how the solution changes between the time instants when it leaves the hyperplane given by $v = C_v\xi = 0$. This occurs when $-L_u\xi = F_S$ or $-L_u\xi = -F_S$. The map is shown in Fig. 10. The symmetry implies that it suffices to study one half of the limit cycle for an odd limit cycle. The Jacobian W of this map thus covers only half a period. For a full period the Jacobian is given by W^2. The following theorem gives the expression for W.

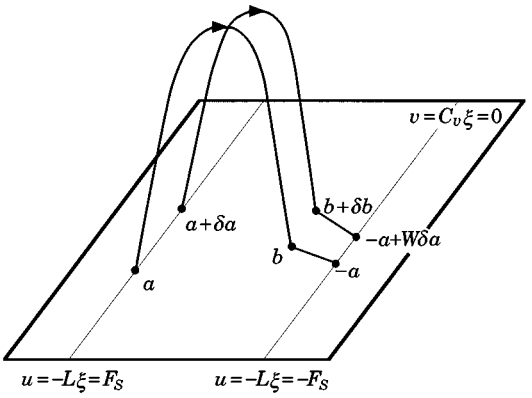

Fig. 10. The Poincaré map describes how the solution changes between the time instants when it leaves a hyperplane given by $v = C_v\xi = 0$. The two lines are determined by $u = -L_u\xi = F_S$ and $u = -L_u\xi = -F_S$. The figure shows the solution when the initial state of the limit cycle is perturbed.

Theorem 3: Assume that an odd periodic solution as described in Theorem 1 exists. The Jacobian W^2 of the Poincaré map, shown in Fig. 10, is then given by

$$W = \left(I - \frac{wL_u}{L_u w}\right)\Phi\left(I - \frac{zC_v}{C_v z}\right)\Phi_c \tag{25}$$

where $z = A_c b - BF_C + B_r y_r$ and $w = -Aa + B_r y_r$. The limit cycle is locally stable if and only if the matrix W has all its eigenvalues inside the unit circle.

Proof: Consider the trajectory resulting from the perturbed initial condition $x(0) = a + \delta a$, see Fig. 10. The perturbation is chosen such that it satisfies the conditions

$$C_v(a + \delta a) = 0$$

and

$$-L_u(a + \delta a) = F_S.$$

Therefore, it lies on the line $-L_u\xi = F_S$ in the hyperplane $C_v\xi = 0$. Assume that the corresponding perturbation of h_1 is δh_1 so that

$$C_v\xi(h_1 + \delta h_1) = 0.$$

Further

$$\begin{aligned} \xi(h_1 + \delta h_1) =& e^{A_c(h_1+\delta h_1)}(a + \delta a) \\ & - \int_0^{h_1+\delta h_1} e^{A_c(h_1+\delta h_1 - s)}dsBF_C \\ & + \int_0^{h_1+\delta h_1} e^{A_c(h_1+\delta h_1 - s)}dsB_r y_r. \end{aligned}$$

Making a series expansion in δa and δh_1, we get

$$\begin{aligned}\xi(h_1+\delta h_1) =&\Phi_c(I+A_c\delta h_1)(a+\delta a)\\ &-(I+A_c\delta h_1)\Gamma_c F_c+(I+A_c\delta h_1)\Gamma_{cr}y_r\\ &-BF_c\delta h_1+B_r y_r\delta h_1+\mathcal{O}(\delta^2)\\ =&\Phi_c a-\Gamma_c F_c+\Gamma_{cr}y_r+\Phi_c\delta a\\ &+A_c(\Phi_c a-\Gamma_c F_c+\Gamma_{cr}y_r)\delta h_1-BF_c\delta h_1\\ &+B_r y_r\delta h_1+\mathcal{O}(\delta^2)\\ =&b+\Phi_c\delta a+(A_c b-BF_c+B_r y_r)\delta h_1\\ &+\mathcal{O}(\delta^2). \end{aligned}\tag{26}$$

Since $C_v b = C_v\xi(h_1+\delta h_1)=0$, we get

$$C_v\Phi_c\delta a=-C_v z\delta h_1+\mathcal{O}(\delta^2).$$

It follows from Remark 1 of Theorem 1 that $C_v z<0$, hence

$$\delta h_1=-\frac{C_v\Phi_c}{C_v z}\delta a+\mathcal{O}(\delta^2).$$

Inserting this in (26) gives

$$\xi(h_1+\delta h_1)=b+\left(I-\frac{zC_v}{C_v z}\right)\Phi_c\delta a+\mathcal{O}(\delta^2).$$

The perturbation at time $t=h_1+\delta h_1$ is thus given by

$$\delta b=\left(I-\frac{zC_v}{C_v z}\right)\Phi_c\delta a+\mathcal{O}(\delta^2).$$

In the same way we can study how the perturbation δb of b affects the solution at the end of the half period, i.e., at time $h_1+\delta h_1+h_2+\delta h_2$. We get

$$\begin{aligned}\xi(h_1+\delta h_1+h_2+\delta h_2) =&e^{A(h_2+\delta h_2)}(b+\delta b)\\ &+\int_0^{h_2+\delta h_2}e^{A(h_2+\delta h_2-s)}dsB_r y_r.\end{aligned}$$

A series expansion gives

$$\begin{aligned}\xi(h_1+\delta h_1+h_2+\delta h_2) =&-a+\Phi\delta b\\ &+(-Aa+B_r y_r)\delta h_2+\mathcal{O}(\delta^2).\end{aligned}$$

Further, it holds that $L_u a=-L_u\xi(h_1+\delta h_1+h_2+\delta h_2)=-F_S$ and from Remark 1 of Theorem 1 we know that $-L_u w<0$, which gives

$$\delta h_2=-\frac{L_u\Phi}{L_u w}\delta b+\mathcal{O}(\delta^2).$$

Finally,

$$\xi(h_1+\delta h_1+h_2+\delta h_2)=-a+\left(I-\frac{wL_u}{L_u w}\right)\Phi\delta b+\mathcal{O}(\delta^2).$$

The Jacobian of the Poincaré map in Fig. 10 is hence given by (25) which proves the theorem. ■

Remark: The matrix W has two eigenvalues at the origin. One comes from $(I-zC_v/C_v z)\Phi_c$ with right eigenvector $\Phi_c^{-1}z$. This removes any perturbation in the velocity at time $h_1+\delta h_1$ caused by δa, i.e., it makes sure that at $t=h_1+\delta h_1$ we are on the hyperplane indicated in Fig. 10. The second zero eigenvalue originates from $(I-wL_u/L_u w)\Phi$ with left eigenvector L_u. It annihilates any remaining perturbation in $\eta(h_1)$, i.e., in the subsystem that is free to move during sticking and implies that at $t=h_1+\delta h_1+h_2+\delta h_2$ we are on the line on the hyperplane as indicated in Fig. 10.

D. Analysis of a Given System

Tools for analyzing a given system have been given. The procedure to determine if a system may have an odd stable periodic solution, as seen in Fig. 2, which is caused by friction of the type (2) is simply:

Step 1) Find h_1, h_2 and e such that $f_1(h_1,h_2,e)=0$, $f_2(h_1,h_2,e)=0$ and $f_3(h_1,h_2,e)=-F_S$.

Step 2) Compute a, b, z, w, and W and check that $C_v z<0$, $-L_u w<0$ and $|\lambda(W)|<1$.

Step 3) Check the conditions $C_v\xi(t)>0$ for $0<t<h_1$ and $|L_u\xi(t)|<F_S$ for $h_1\le t<h_1+h_2$.

Complete procedures have now been given for the exact analysis of friction generated limit cycles of the type shown in the upper curve of Fig. 2. In the next section they are applied to the example in Section II-A.

IV. Application to Servo System

The results from the previous section will now be applied to the servo example in Section I. The tools have been implemented in Matlab, where the zeros of the functions are found using a Newton–Raphson method.

The flexible servo in Section I showed different limit cycles depending on the design parameter ρ.

For $\rho=10$, the simulations showed no limit cycle. Accordingly, a numerical solution for h_1, h_2, and e failed which confirms the simulations.

An odd limit cycle with sticking occured when simulating the flexible servo for $\rho=11$. A numerical solution gives $h_1=0.1357$, $h_2=0.0465$, and $e=-0.00281$. The magnitude of the largest eigenvalue of the Jacobian W is 0.618. The limit cycle is thus stable and with moderate convergence rate. The derivatives of the velocity and the control signal has the correct sign at times $t=h_1$ and $t=h_1+h_2$, respectively. Fig. 11 shows a simulated period using initial conditions corresponding to the limit cycle.

The oscillation for $\rho=12$ is of relay type and can, therefore, be analyzed with the tools in [5]. A numerical solution gives $h=0.157$, which is half the period. The largest eigenvalue of the Jacobian W has magnitude 0.573, which assures stability. A simulation of one period with initial conditions corresponding to the limit cycle is shown in Fig. 12.

If ρ is increased to five, the oscillation in the velocity becomes more sinusoidal. Half the period is given by $h=0.127$ and the largest eigenvalue of the Jacobian has magnitude 0.5054. The convergence to the limit cycle is thus faster with larger values of ρ. Fig. 13 shows the velocity and the control signal for one period.

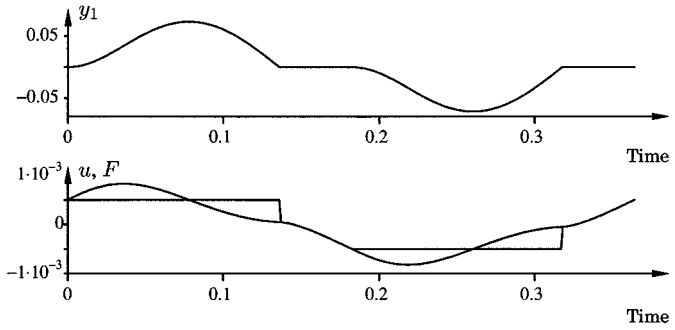

Fig. 11. Simulation of the periodic solution for the flexible servo when $\rho = 11$. The initial conditions are determined numerically using the implemented tools.

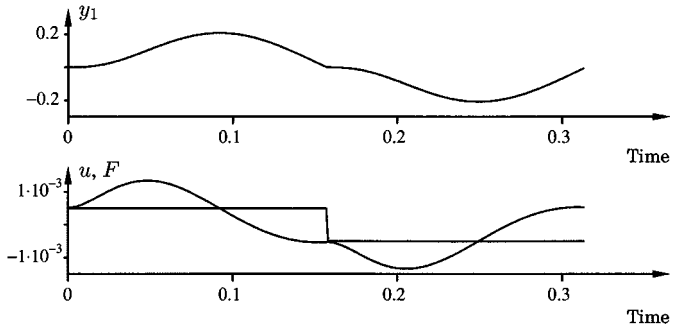

Fig. 12. Simulation of the periodic solution for the flexible servo when $\rho = 12$. The initial conditions are determined numerically using the implemented tools.

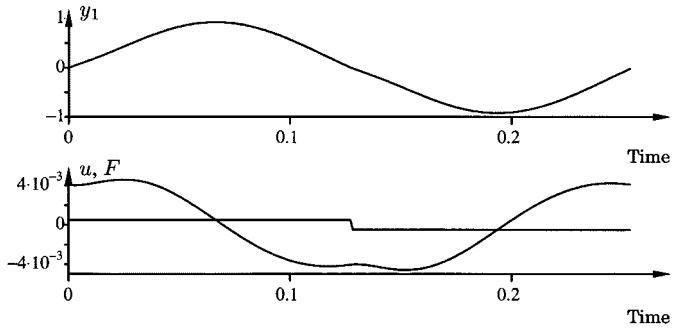

Fig. 13. Simulation of the periodic solution for the flexible servo when $\rho = 15$. The initial conditions are determined numerically according to the procedure for relay oscillations.

The procedure developed has thus demonstrated its ability to analyze friction generated limit cycles. The example has shown that in particular for limit cycles with large periods of sticking they give a much more accurate prediction than decribing function analysis would do.

V. Conclusion

We have in this paper discussed limit cycles generated by friction. An example has demonstrated oscillations that may occur and also different natures of the limit cycles. The oscillations have been characterized. It is necessary to distinguish between limit cycles with and without periods of sticking. If sticking does not occur, the limit cycles are equivalent to pure relay oscillations and can be analyzed as such. The tools available for relay oscillations have then been extended to limit cycles with sticking. The tools are suitable for numerical determination of possible limit cycles. The example has been analyzed using the derived numerical methods.

References

[1] A. Wallenborg and K. J. Åström, "Limit cycle oscillations in high performance robot drives," in Preprints Control '88, U.K., 1988.

[2] H. Olsson, K. J. Åström, C. C. de Wit, M. Gäfvert, and P. Lischinsky, "Friction models and friction compensation," *European J. Contr.*, vol. 3, pp. 176–195, 1998.

[3] Z. T. Tsypkin, *Relay Control Systems*. Cambridge, U.K.: Cambridge Univ. Press, 1984.

[4] D. P. Atherton, "Limit cycles in relay systems," *Electron. Lett.*, vol. 18, no. 21, p. 922, 1982.

[5] K. J. Åström, "Oscillations in systems with relay feedback," in *Adaptive Control, Filtering and Signal Processing*, K. J. Åström, G. C. Goodwin, and P. R. Kumar, Eds: Springer-Verlag, 1995.

[6] P. A. Derek, *Nonlinear Control Engineering—Describing Function Analysis and Design*. London, U.K.: Van Nostrand Reinhold, 1975.

[7] K. H. Johansson, A. Rantzer, and K. J. Åström, "Fast switches in relay feedback systems," *Automatica*, vol. 35, no. 4, pp. 539–552, 1999.

[8] H. Olsson, "Control Systems with Friction," Ph. D. dissertation, Dept. Automat. Contr., Lund Inst. Technol., Lund, Sweden, 1996.

[9] C. F. Abelson, "The effect of friction on stabilization of an inverted pendulum," Master thesis, Dept. Automat. Contr., Lund Inst. Technol., Lund, Sweden, 1996.

[10] M. Gäfvert, "Comparisons of two dynamic friction models," in *Proc. 6th IEEE Conf. Contr. Applicat. (CCA)*, Hartford, CT, Oct. 1997.

[11] ——, "Department of Automatic Control, Lund Institute of Technology," Master, Lund, Sweden, 1996.

[12] A. Wallenborg, "Control of Flexible Servo Systems," Lic. tech. thesis, Dept. Automat. Contr., Lund Inst. Technol., Lund, Sweden, 1987.

[13] K. H. Johansson, "Relay Feedback and Multivariable Control," Ph. D. dissertation, Dept. Automat. Contr., Lund Inst. Technol., Lund, Sweden, 1997.

[14] H. K. Khalil, *Nonlinear Systems* Macmillan, New York, 1992.